NMR Studies on Effects of Tetraalkylammonium Bromides on Micellization of Sodium Dodecyl Sulfate.

3 **AUTHORS**, INCLUDING:

Jia-Hsien Lin
National Cheng Kung University

**5** PUBLICATIONS   **49** CITATIONS

NMR Studies on Effects of Tetraalkylammonium Bromides on Micellization of Sodium Dodecylsulfate

Jia-Hsien Lin, Wen-Shan Chen, and Sheng-Shu Hou*

Department of Chemical Engineering, National Cheng Kung University, Tainan 70101, Taiwan

Ⓢ Supporting Information

ABSTRACT: The effects of tetraalkylammonium bromides (TAABs) on the micellization of sodium dodecylsulfate (SDS) are studied using pyrene solubilization and several nuclear magnetic resonance (NMR) techniques. Two-dimensional nuclear Overhauser effect spectroscopy (2D NOESY) experiments confirm that tetraalkylammonium (TAA$^+$) ions associate with SDS to form mixed micelles. TAA$^+$ ions attach to the surface of the mixed micelles and become inserted into the hydrophobic core of the mixed micelles. Because TAA$^+$ ions appear in the hydrophobic interior of the TAA-SDS mixed micelles, the micropolarity inside the mixed micelles sensed by pyrene might not reflect the true hydrophobicity of the micellar core. Using proton chemical shift analysis, the degree of hydration on the surface of the mixed micelles is determined from the chemical shift change of SDS α-CH$_2$ protons. The self-diffusion coefficients of SDS and TAA$^+$ ions in the TAAB/SDS/D$_2$O solutions are measured by using pulse-field gradient NMR, and the fraction of TAA$^+$ ions associated with the SDS to form the mixed micelles is calculated from the self-diffusion data. Moreover, secondary micelle formation for SDS and TAA$^+$ ions is observed on the basis of ^{1}H chemical shift analysis and the self-diffusion data. The 2D NOESY experiments also reveal unusual tumbling behavior of SDS alkyl protons. For Pr$_4$NBr/SDS and Bu$_4$NBr/SDS solutions, positive and negative nuclear Overhauser effects are simultaneously observed among the SDS alkyl protons.
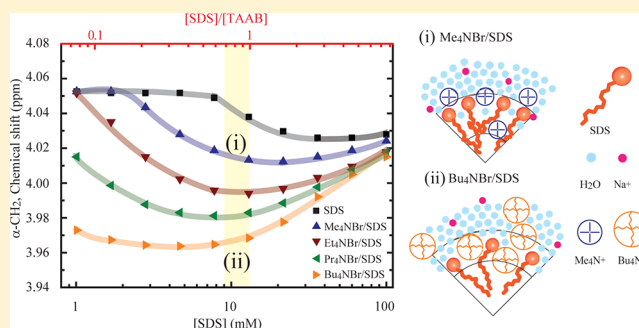
INTRODUCTION

Micellization is a feature of surfactant solutions and plays an important role in some interfacial phenomena such as solubilization, emulsion, and detergency. In many situations, surfactants are added in the presence of inorganic or organic salts in the solutions.[1−4] Therefore, understanding the micellization of surfactants in the presence of salts is of considerable importance since the salt effects on the micellization process can be very striking.

Surfactant molecules self-assemble into micelles when the surfactant concentration exceeds the critical micelle concentration (cmc). For ionic surfactants, micelle formation is the physical result of the interplay between favorable interactions of hydrophobic tails and retardant electrostatic repulsion from charged headgroups. The presence of charged species in surfactant solutions can thus potentially affect the micellization process through specific interactions with the surfactant molecules. The greatest effect caused by an inorganic electrolyte is to decrease the cmc of a surfactant, which is primarily due to a reduction in the electrostatic repulsion among headgroups of surfactant molecules. It has been shown that the effectiveness of the added inorganic ions at lowering the cmc of a surfactant is qualitatively related to the hydrated radius of the counterions.[5,6] In general, the smaller the extent of hydration of the ion, the greater is its affinity to the headgroup of a surfactant molecule. An inorganic cation with a small hydrated radius is more difficult to be hydrated as compared to that with a large hydrated radius. When the radius of a counterion is smaller, the counterion is more hydrated by water molecules with a stronger ion-dipole force; thus, the small counterion is almost surrounded by water molecules, which weakens its ability to separate the charge of the headgroup.

In addition to reducing the cmc, the addition of organic salts into ionic surfactant solutions significantly impacts the characteristics of micelles and the solution properties.[7−12] The impact is due to the water structure and counterion distribution in the hydration layer around micelles being disrupted by the hydrophobic part of the bound organic ions. Recently, the effect of tetraalkylammonium (TAA$^+$) ions on the micellization of anioinic surfactants has attracted some interest because it causes the cloud point phenomenon, which is uncommon with anionic surfactants.[13−16] Some 1:1 tetraalkylammonium sulfates have been synthesized to study the roles of counterions in micelle aggregation behavior and micellar properties.[16−21] Additionally, the interations between tetraalkylammonium bromides (TAABs) and sodium (or lithium) dodeylsulfate (SDS) have been studied by conductivity, surface tension, and calorimetry.[22−24] These studies, however, focused

on the bulk solution properties of the mixed TAABs/surfactant solutions. The detailed association behaviors between SDS and TAA$^+$ ions still remain unexplored on the molecular level.

The present study first uses pyrene solubilization to understand and quantify the extent of the interaction between TAABs and SDS as a function of SDS concentration. Figure 1
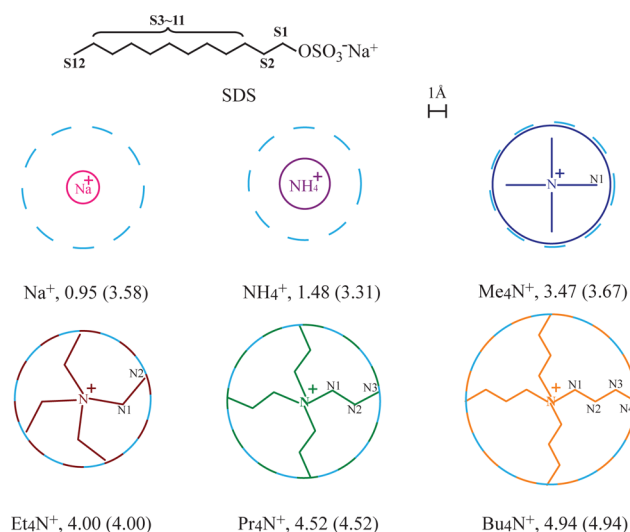

Figure 1. Chemical structures of SDS and TAA$^+$ ions. The dashed-line circle indicates the effective size of the hydration shell. The values below the structures are the ionic and hydrated radii of the ions.[25]

shows the chemical structures of the four TAA$^+$ ions under investigation and their ionic and hydrated radii.[25] Nuclear magnetic resonance (NMR) spectroscopy is a unique and powerful tool for obtaining intrinsic atomic-level structural information. The binding affinity of TAA$^+$ ions to micelles and the inner structure of a micelle are studied using various NMR techniques, namely chemical shift analysis, pulse-field gradient (PFG) NMR, and two-dimensional nuclear Overhauser effect spectroscopy (2D NOESY). The results indicate that TAABs and SDS form mixed micelles and that the surface hydration of the mixed micelles is correlated closely with the size and hydrophobicity of TAA$^+$ ions.

EXPERIMENTAL SECTION

Chemicals. SDS (Aldrich, 99%) and pyrene (Merck, >97%) were recrystallized twice from methanol and then dried under vacuum at 50 °C to remove residual solvent. Tetraalkylammonium bromides (R$_4$NBr, R = CH$_3$, C$_2$H$_5$, C$_3$H$_7$, and C$_4$H$_9$) were purchased from Alfa Aesar (>98%) and used as received. Deuterium oxide (99.9%) was purchased from Aldrich.

Pyrene Solubilization Experiments. Pyrene was used as the probe to detect micropolarity in the interior of a micelle. Pyrene-saturated aqueous solutions were prepared as follows. About 3.0 mg of pyrene was added into 500 mL of deionized water. After this solution was stirred for more than 24 h at room temperature in the dark, insoluble pyrene was removed by filtration. The concentration of pyrene in pyrene-saturated water is 1.0×10^{-6} M. TAAB/SDS solutions were prepared by mixing the concentrated mother solutions using pyrene-saturated water, and then diluted to the desired concentrations. All the samples were kept at room temperature in the dark for 24 h before measurements. The emission fluorescence spectra of pyrene were measured on a F2500 spectrofluorometer (Hitachi) at an excitation wavelength of 332.0 nm. The slit widths were set at 10 nm for excitation and at 2.5 nm for emission. The I_1/I_3 ratio was calculated as the ratio of the intensity of peak I_1 (374.0 nm) to that of peak I_3 (385.0 nm) of the vibration fine structure of pyrene monomer emission.

NMR Experiments. The NMR experiments were performed at 303.0 K on a Bruker Avance-500 spectrometer equipped with a Bruker 5 mm BBO 500 MHz Z-gradient high-resolution probe at a proton resonance frequency of 500.13 MHz. All NMR data were processed using the software package Bruker Topspin 2.1. For each sample, the one-dimensional ^{1}H NMR spectrum was acquired using the standard Bruker pulse program zg30. The 90° pulse was 11.2 μs and the relaxation delay was 2 s. A total of 128 transients were acquired into 64k data points using a spectral width of 7500 Hz and an acquisition time of 4.67 s. The proton chemical shifts were determined relative to an external standard DSS (4,4-dimethyl-4-silapentane-1-sulfonic acid) solution (0.5 wt % in D$_2$O) in a coaxial tube with DSS being at δ = 0.00 ppm.

The self-diffusion coefficients of TAA$^+$ ions and SDS were measured by PFG NMR spectroscopy using the bipolar pulse pair longitudinal-eddy-current delay (BPPLED) pulse se-
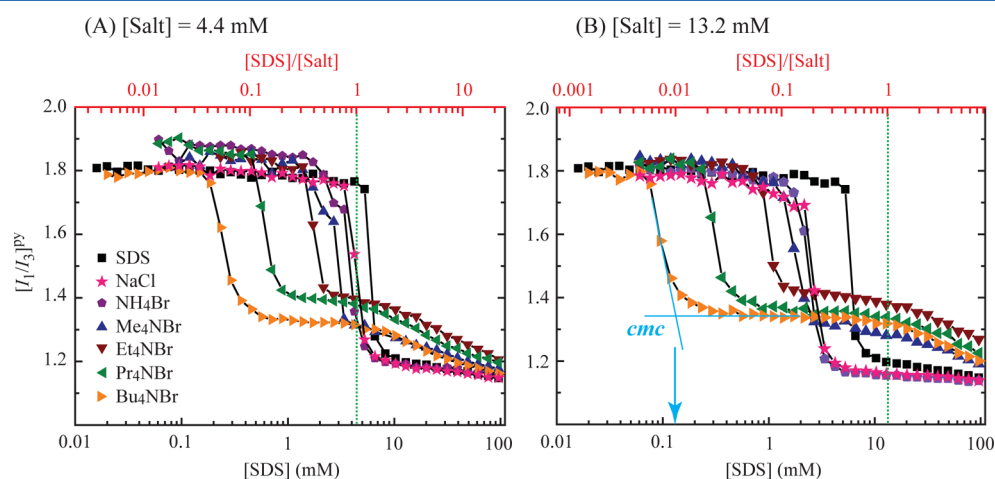

Figure 2. Plots of pyrene I_1/I_3 as a function of SDS concentration for TAAB/SDS solutions. The salt concentrations are (A) 4.4 and (B) 13.2 mM. The cmc is defined at the inflection point of the I_1/I_3 curve, as indicated.

quence.[26] An eddy current delay of 5.0 ms was incorporated in the pulse sequence to avoid the spectral artifacts from the residual eddy current. The length of diffusion time (Δ) was optimized for each sample (50−100 ms). With the gradient duration (δ) fixed, the strength of the two pairs of 3.0 ms bipolar square gradients was varied from 2 to 95% in 16 linear increments. The maximum gradient was about 0.40 T/m. The delay for gradient recovery (τ) was 0.2 ms. The diffusion coefficients were calculated using the nonlinear least-squares method based on the following equation:

$$I = I_0 \exp[-D\gamma^2 g^2 \delta^2 (\Delta - \delta/3 - \tau/2)]$$

where I is the attenuated intensity of the NMR signal, I_0 is the intensity of the NMR signal in the absence of the gradient pulse, D is the diffusion coefficient, and γ is the magnetogyric ratio.

The 2D NOESY spectra were acquired with the standard pulse program ($90°-t_1-90°-t_m-90°$ acquisition). The NOESY program was run with a 11.2 μs 90° pulse, a 200 ms mixing time, a 1.5 s relaxation delay, and a 4.7 kHz spectral window. A total of 32 transients were averaged for each of the 256 t_1 increments using time proportional phase incrementation (TPPI) detection. The FID was treated by square-shifted sine bell weighting functions in both dimensions.

■ RESULTS AND DISCUSSION

Pyrene Solubilization Experiments. Pyrene fluorescence was first used to determine the cmc of SDS in the presence of the four symmetrical TAABs (Me$_4$NBr, Et$_4$NBr, Pr$_4$NBr, and Bu$_4$NBr). In Figure 2, the intensity ratios (I_1/I_3) of monomeric pyrene emission at 374 and 385 nm are plotted as a function of [SDS] in the presence of 4.4 mM (Figure 2A) and 13.2 mM (Figure 2B) TAABs. The I_1/I_3 value is proportional to the microenvironment polarity at pyrene molecule locations. The smaller the I_1/I_3 value, the greater is the hydrophobicity of the microenvironment. The cmc of the surfactant can thus be determined by plotting the I_1/I_3 ratio as a function of the surfactant concentration. The concentrations of TAABs used in this study are far below their regular cmc.[27,28] For comparison, the I_1/I_3 curves for two inorganic salts, sodium chloride (NaCl) and ammonium bromide (NH$_4$Br), are also included. All the I_1/I_3 curves have a similar profile, in which the I_1/I_3 value remains near the surfactant-free value ($I_1/I_3 = {\sim}1.8-1.9$) until the cmc and then decreases abruptly to a lower plateau value. The cmc of the mixed TAAB/SDS solutions is defined at the inflection point of the I_1/I_3 curve, as illustrated in Figure 2B. The surface tension method was also used to determine the cmc of the TAAB/SDS solutions. The cmc values measured by the surface tension method are almost the same as those obtained in the pyrene solubilization experiments. The cmc values of all the mixed solutions of SDS and TAABs are summarized in Table 1.

Figure 2 and Table 1 indicate that the cmc of SDS decreases with increasing alkyl chain length of TAABs. In addition, the decrease of cmc of SDS in the presence of TAABs is much more pronounced than that with the added inorganic salts. The dramatic reduction of SDS cmc in the presence of TAABs is due to the negative charge of the SDS headgroup attracting TAA$^+$ ions by electrostatic interactions, and thus, the unfavorable repulsive electrostatic interactions among the SDS headgroups are screened out. Furthermore, the hydrophobic interactions between TAA$^+$ ions and SDS molecules

Table 1. cmc Values of TAAB/SDS Solutions and Micropolarity in the Mixed Micelles

salt	[salt] = 4.4 mM		[salt] = 13.2 mM	
	cmc^a (mM)	micropolarity^b (I_1/I_3)	cmc^a (mM)	micropolarity^b (I_1/I_3)
	8.0 (7.0)	1.18	8.0 (7.0)	1.18
NaCl	5.5 (5.0)	1.17	3.5 (3.9)	1.15
NH$_4$Br	5.0 (5.0)	1.18	3.1 (3.2)	1.15
Me$_4$NBr	3.4 (3.8)	1.24	2.4 (2.0)	1.26
Et$_4$NBr	2.2 (2.4)	1.30	1.2 (1.2)	1.35
Pr$_4$NBr	0.8 (1.0)	1.28	0.4 (0.5)	1.32
Bu$_4$NBr	0.3 (0.2)	1.22	0.1 (0.1)	1.29

^{a}The cmc values in parentheses were measured by the surface tension method. ^{b}The I_1/I_3 values were taken at [SDS] = 25 mM.

make TAA$^+$ ions preferentially bind tightly on the surface of the SDS micelle or even become inserted into the micellar interior, forming TAA-SDS mixed micelles. The formation of TAA-SDS mixed micelles is further supported by NMR studies, which are explained in more detail in the following sections. It should be noted that local turbidity was observed in the initially concentrated stage during the preparation of some Bu$_4$NBr/SDS samples, but the precipitate was dissolved very fast on dilution and the mixed solutions became completely transparent.[22] Therefore, coacervation involving Bu$_4$N$^+$ ions and SDS in the concentrated Bu$_4$NBr/SDS mixed solutions is possible.[29] However, the concentration of Bu$_4$NBr in the final solution under investigation in the present study are sufficiently low (<0.5 wt %) so that only the micellar phase exists in all of the samples under investigation.

Pyrene fluorescence not only gives the cmc but also provides information on the interior structure of the TAA-SDS mixed micelles. It can be seen in Figure 2 that for the SDS solutions containing NaCl and NH$_4$Br, the lower I_1/I_3 plateau value is smaller than that for pure SDS solution. This means that the interior of an SDS micelle with added NaCl or NH$_4$Br is more hydrophobic than that of a salt-free SDS micelle. The lower plateau I_1/I_3 values for the mixed TAAB/SDS solutions, however, never fall below the characteristic value for pure SDS micelles. The I_1/I_3 values for the solutions with the added TAABs at [SDS] = 25 mM are listed in Table 1. They are found to decrease in the order Et$_4$NBr > Pr$_4$NBr > Bu$_4$NBr $\cong$ Me$_4$NBr. These results are consistent with the order obtained for tetraalkylammonium dodecylsulfates (1:1 salts).[17] It seems to be reasonable to assume that the core of TAA-SDS mixed micelles is more polar than that of pure SDS micelles. However, some studies have indicated that there is an attractive interaction resulting from the π-electrons of pyrene and the positive charge of the quaternary ammonium group.[30−32] Pyrene molecules are therefore supposed to be located preferentially near the surface of the TAA-SDS mixed micelles, which is more polar than the core. Consequently, the higher I_1/I_3 values for TAA-SDS mixed micelles do not necessarily indicate that their core is more hydrophilic.

The most notable feature of the I_1/I_3 curves for the four TAAB/SDS solutions is that there is a discontinuous break in the lower I_1/I_3 plateau. This break is at an [SDS]/[TAAB] ratio of about one regardless of the TAAB concentration, as shown by the dashed lines in Figure 2. Although the I_1/I_3 value cannot really reflect the micropolarity inside the TAA-SDS mixed micelles, this break strongly suggests that the structure of the
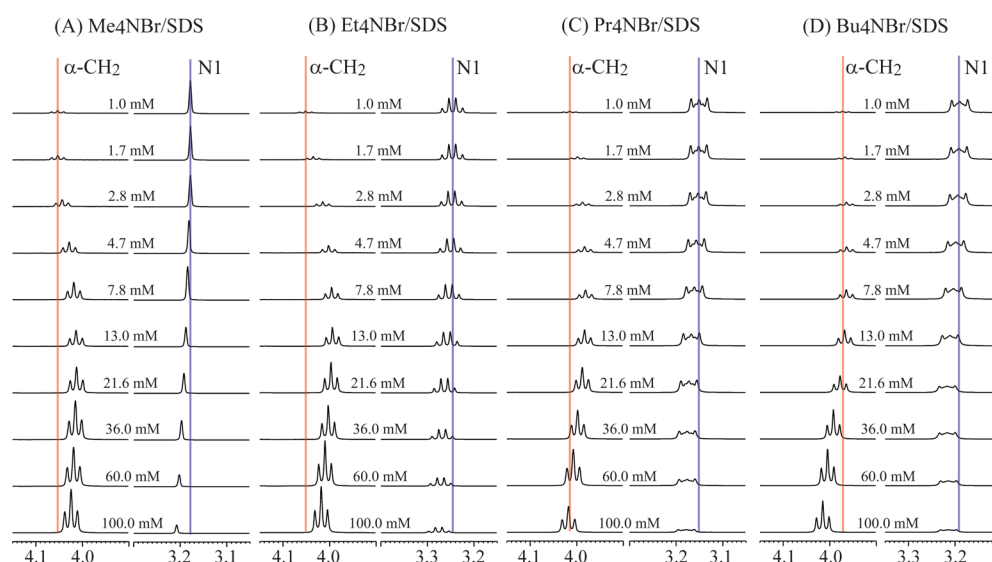
Figure 3. Cropped ^1H NMR spectra of (A) Me$_4$NBr/SDS, (B) Et$_4$NBr/SDS, (C) Pr$_4$NBr/SDS, and (D) Bu$_4$NBr/SDS. [TAAB] = 13.2 mM.

TAA-SDS mixed micelles varies with the amount of TAA$^+$ ions associated with SDS.

Chemical Shift Analysis and Hydration of Mixed Micelles. Chemical shift analysis has been proven to be an efficient tool for investigating micelle formation in aqueous solution.[33−37] ^1H NMR chemical shifts sensitively reflect nearest-neighbor and next-nearest-neighbor environments of the nuclei. The proton chemical shift provides information about the local chemical environment at the micellar surface and in the palisade layer, which consists of the first few carbon atoms of the hydrophobic groups that comprise the outer core of the micellar interior. When SDS molecules associate to form a micelle, the head groups of SDS monomers repel one another; therefore, during micellization, the chemical shift of α-methylene protons attached to the sulfate group is significantly affected by the charge distribution around the sulfate group. Figure 3 shows the cropped one-pulse ^1H NMR spectra of the mixed TAAB/SDS solutions for various SDS concentrations.

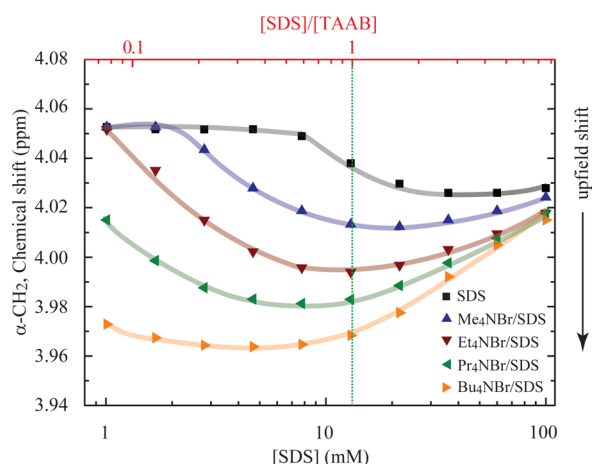Figure 4 shows the trend of change in chemical shifts for α-methylene protons as a function of SDS concentration. In principle, the observed chemical shift of SDS protons is a mole fraction weighted average of contributions from free and micellar states. For pure SDS solution, when [SDS] is smaller than the regular cmc, the chemical shift of α-CH$_2$ remains a constant (δ = 4.053 ppm), which can be regarded as the reference chemical shift of α-CH$_2$ of free SDS monomer in water. After micellization, the chemical shift of α-CH$_2$ shows a significant upfield shift and then converges to a steady value (δ = 4.028 ppm), which reflects the chemical environment of α-CH$_2$ in a pure SDS micelle.

The variation of the chemical shift of α-CH$_2$ with SDS concentration in the presence of TAABs is different from that for pure SDS. A much larger upfield shift of α-CH$_2$ was observed when SDS molecules formed mixed micelles with the added TAA$^+$ ions. The upfiled shift was more pronounced for TAABs with longer alkyl groups. When the SDS concentration was increased further, the chemical shift of α-CH$_2$ reached a minimum. Then, the chemical shift of α-CH$_2$ exhibited gradual downfield shifting. At [SDS] = 100 mM, the shift was close to the value of α-CH$_2$ for a pure SDS micelle. The minimum value for the chemical shift of α-CH$_2$ occurs at [SDS]/[TAAB] = 0.30 for Bu$_4$NBr, 0.55 for Pr$_4$NBr, 0.75 for Et$_4$NBr, and 1.20 for Me$_4$NBr.

The changes in the chemical shift of SDS α-CH$_2$ can be interpreted in terms of the charged species surrounding the sulfate group. According to quantum-chemical calculations, α-CH$_2$ is partially positive and can be regarded as part of the sulfate group.[38] For the pure SDS solution, the upfield shift shown by α-CH$_2$ after micellization indicates that the SDS α-CH$_2$ protons in the SDS micelle are more shielded than those of the SDS monomers in water. When the SDS molecule is in the monomeric state, the sulfate group is completely surrounded by water and its counterions (Na$^+$). In contrast, the sulfate group of SDS in the micelle is only in partial contact with hydrated water molecules and Na$^+$ ions. The negative charge of the sulfate group in the micelle, as compared to that in the monomeric state, is therefore less covered by fewer water molecules and Na$^+$ ions in the hydration layer. Consequently, the α-CH$_2$ protons are more shielded by the more negative sulfate group in the micelle, which gives rise to the observed upfield shift.

Figure 4. Variation in chemical shifts for α-methylene protons of SDS as a function of SDS concentration. The upfield shifts of SDS α-CH$_2$ are related to the degree of dehydration on the surface of the mixed micelles. A larger upfield shift indicates a more hydrophobic surface.

For the SDS solution containing 13.2 mM TAABs, the more significant upfield shift of α-CH_2 is due to the tightly bound TAA^+ ions on the surface of the mixed micelle. When the TAA^+ ions are attached to the micellar surface, water and Na^+ on the micellar surface are depleted by the hydrophobic alkyl groups of TAA^+ ions. The number of water molecules and Na^+ ions, which are in direct contact with the sulfate group, condensed in the hydration layer of a TAA-SDS mixed micelle is much lower than that on the surface of a pure SDS micelle, as illustrated in Figure 5. In other words, the surface of a TAA-SDS mixed
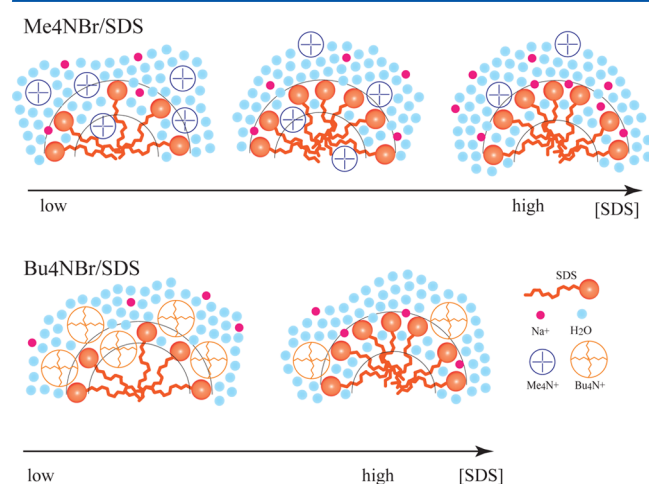

Figure 5. Illustration of biding of Me_4N^+ and Bu_4N^+ on the micllar surface and in the palisade layer. Based on the results of 2D NOESY experiments, some Me_4N^+ ions are located in the center of the mixed micelle and Bu_4N^+ ions are mostly located in the palisade layer.

micelle becomes hydrophobic and is resistant to hydration by water and Na^+ ions. Additionally, the more hydrophobic TAA^+ ions bind more tightly on the micellar surface and the hydration layer is reduced to a greater extent. As a result, the most dramatic upfield shift of α-CH_2 is observed in the Bu_4NBr/SDS solutions.

For the mixed TAAB/SDS solutions, at a certain SDS concentration, the chemical shift of α-CH_2 begins to shift to the downfield from the minimum value. At this minimum SDS concentration, the number of TAA^+ ions bound on the micellar surface reaches its maximum. As the ratio of [SDS]/[TAAB] increases, there will be more SDS molecules on the surface of the mixed micelle, which are not bound with TAA^+ ions. These uncovered SDS molecules are hydrated by water and Na^+ ions. Therefore, the chemical shift of α-CH_2 moves to the downfield again as the SDS concentration further increases.

Similarly, the opposite variation in chemical shifts can be observed from the aspect of TAA^+ ions, as shown in Figure 3. The free TAA^+ ions are completely surrounded by water and Br^-, whereas the bound TAA^+ ions in the mixed micelles are only partially hydrated. Thus, the bound TAA^+ ions should be more positive than the free TAA^+ ions, because they are less neutralized by water and Br^-. As a result, the chemical shift of the methylene protons bonded to the nitrogen atom (N1) should show a downfield shift.

Binding Affinity of TAABs in Mixed Micelles. The results from pyrene solubilization and chemical shift analysis indicate that micropolarity in the micelle and surface hydration of the mixed micelle strongly depend on the [SDS]/[TAAB] ratio. The binding affinity between TAA^+ ions and the sulfate

group can explain these concentration-dependent behaviors. In order to evaluate the binding affinity of TAA^+ ions to SDS in the mixed micelles, PFG NMR was used to measure the self-diffusion coefficients of TAA^+ ions and SDS.[39,40] The time scale of PFG NMR is longer than to the exchange rate of the free and micelle-bound SDS molecules (or TAA^+ ions). Thus, the self-diffusion coefficient (D_{obs}) of SDS molecules and TAA^+ ions measured by PFG NMR is a time-averaged value of the free (D_f) and micellar (D_m) states with the fractions denoted by ($1 - f_m$) and f_m, respectively:

$$D_{obs} = (1 - f_m)D_f + f_m D_m$$

The diffusion coefficients of SDS and TAA^+ ions, which were calculated from the attenuation of the α-CH_2 signal of SDS (D_{SDS}) and from the protons on the carbon (N1 protons) directly bonded to nitrogen for TAA^+ ions (D_{TAA+}), respectively. A free SDS self-diffusion coefficient ($D_{SDS,free}$) of 6.13×10^{-10} m^2/s was measured and averaged for the SDS solutions of [SDS] < 3.0 mM. In the SDS concentration range where the intermicellar interactions are not too large, a micellar SDS self-diffusion coefficient ($D^0_{SDS,mic}$) of 0.56×10^{-10} m^2/s, which can be used to calculate the hydrodynamic radius of the micelles, was obtained by extrapolating the plot of $D_{SDS,mic}$ versus [SDS] at the SDS cmc.[41-43] In addition, the micellar self-diffusion coefficient of TAA^+ ions is assumed to be equal to $D_{SDS,mic}$. The fractions of TAA^+ ions and SDS molecules in the micellar state can be calculated from the time-averaged self-diffusion data and are summarized in Table 2.[44,45]

In Figure 6, the diffusion coefficients for SDS and TAA^+ ions in the mixed SDS/TAAB solutions are plotted as a function of SDS concentration. For the pure SDS solution, the self-diffusion coefficient of SDS (D_{SDS}) is constant up to the regular SDS cmc. When the SDS concentration is higher than its regular cmc, the D_{SDS} decreases rapidly on account of the slower translational movement of SDS micelles.

The self-diffusion coefficient of SDS for the Me_4NBr/SDS solution ($D_{SDS(Me)}$, blue solid line in Figure 6) starts to decrease dramatically at [SDS] = 2–3 mM, which corresponds to the cmc of SDS with added Me_4NBr. The result is consistent with that obtained from the surface tension and pyrene solubilization experiments. Additionally, there is a clear inflection break at [SDS]/[Me_4NBr] = ~1 ([SDS] = 13–14 mM), suggesting the presence of a second structure of the micelle at secondary micelle concentration (cmc-II) for SDS with Me_4NBr.[39] It is worth to note that this inflection break can be correlated with the minimum chemical shift of α-CH_2 (Figure 4). Combination of the results from self-diffusion and chemical shift analysis shows that the cmc-II of SDS with Me_4NBr is around 10–20 mM, which is much lower relative to that (~70 mM) of the pure SDS.[39] The observation of cmc-II is due to the increase in the degree of hydration of the Me_4N^+-SDS mixed micelles.[46] It can be understood as [SDS]/[Me_4NBr] > 1, not all of SDS molecules in the mixed micelles are bound with Me_4N^+ and these uncovered SDS molecules are hydrated by water and Na^+ ions. Thus, a micellar structural transition is obtained also by increasing the SDS concentrations.

The $D_{Me_4N^+}$ value of free Me_4N^+ is 11.65×10^{-10} m^2/s, which is larger than the D_{SDS} value of free SDS monomer. $D_{Me_4N^+}$ (blue dashed line) does not decrease significantly until [SDS] = ~5 mM and is always larger than $D_{SDS(Me)}$ over the full range of SDS concentrations, indicating that the average translational motion of Me_4N^+ (bound and free) is faster than that of the

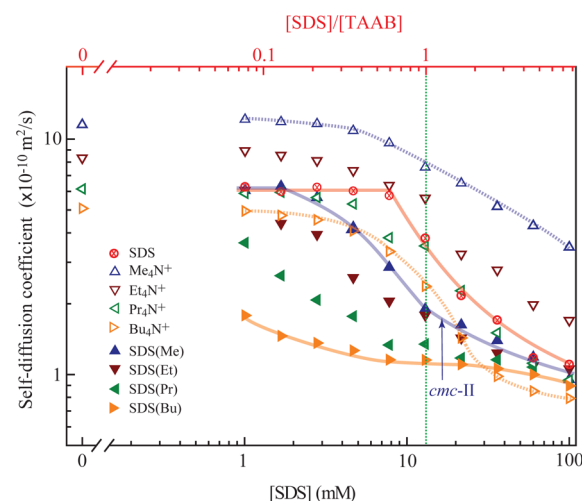**Table 2. Self-Diffusion Coefficients of SDS and TAA$^+$ in TAAB/SDS Solutions**

composition	[SDS] (mM)	D_{SDS}^{a} (10^{-10} m^2/s)	D_{R4N^+} (10^{-10} m^2/s)	$f_{m,R4N^+}$^{b}	$f_{m,SDS}$
SDS/ Me$_4$NBr	0		11.65		
	1.0	6.06	12.12		
	1.7	6.30	11.83		
	2.8	5.65	11.60		
	4.7	4.15	10.85	0.07	0.36
	7.8	2.85	9.62	0.18	0.59
	13.0	1.90	7.59	0.37	0.76
	21.6	1.63	6.50	0.46	0.81
	36.0	1.39	5.17	0.58	0.85
	60.0	1.19	4.28	0.66	0.89
	100.0	0.95	3.47	0.74	0.93
SDS/ Et$_4$NBr	0		8.65		
	1.0	6.07	8.94		
	1.7	4.39	8.55		
	2.8	3.94	8.12	0.07	0.39
	4.7	2.59	7.36	0.16	0.64
	7.8	2.05	6.38	0.28	0.73
	13.0	1.79	5.62	0.37	0.78
	21.6	1.43	3.25	0.67	0.84
	36.0	1.24	2.78	0.73	0.88
	60.0	1.09	1.98	0.82	0.90
	100.0	1.06	1.70	0.86	0.91
SDS/ Pr$_4$NBr	0		6.14		
	1.0	3.63	5.89		
	1.7	2.63	5.94	0.03	0.63
	2.8	2.07	5.64	0.09	0.73
	4.7	1.77	5.30	0.15	0.78
	7.8	1.33	3.81	0.42	0.86
	13.0	1.35	3.52	0.47	0.86
	21.6	1.18	2.27	0.69	0.89
	36.0	1.16	1.50	0.83	0.89
	60.0	1.08	1.12	0.90	0.91
	100.0	0.94	0.95	0.93	0.93
SDS/ Bu$_4$NBr	0		5.08		
	1.0	1.78	4.95	0.03	0.78
	1.7	1.46	4.74	0.08	0.84
	2.8	1.36	4.54	0.12	0.86
	4.7	1.27	4.07	0.22	0.87
	7.8	1.16	3.33	0.39	0.89
	13.0	1.15	2.37	0.60	0.89
	21.6	1.10	1.43	0.81	0.90
	36.0	1.06	0.98	0.91	0.91
	60.0	1.00	0.85	0.94	0.92
	100.0	0.90	0.79	0.95	0.94

^{a}$D_{SDS,free}$ = 6.13 × 10^{-10} (m^2/s) and $D_{SDS,mic}$ = 0.56 × 10^{-10} (m^2/s). ^{b}The concentration of TAABs in the solution was fixed at 13.2 mM.

Figure 6. Apparent self-diffusion coefficients (D_{obs}) of TAA$^+$ ions and SDS in the TAAB/SDS mixed solutions as a function of SDS concentration. The concentration of TAA$^+$ ions is constant at 13.2 mM. The open triangles at [SDS] = 0 represent the self-diffusion coefficients of free TAA$^+$ ions in the absence of SDS.

(orange solid line) decreases slowly until [SDS] = 10 mM, and then levels off when [SDS] = 6−7 mM. This inflection break is the cmc-II for SDS with Bu$_4$NBr. It can be seen in Figure 6 that the cmc-II of SDS with TAAB is decreased as the molecular size of TAAB becomes larger. This can be explained that saturation of the Bu$_4$N$^+$ ions with SDS occurs at a lower SDS concentration, because Bu$_4$N$^+$ has a larger size and is more hydrophobic. $D_{Bu_4N^+}$ (orange dashed line) starts decreasing significantly from the value of the free state when [SDS] > 3 mM. There is a crossover between $D_{SDS(Bu)}$ and $D_{Bu_4N^+}$ when [SDS] > 25 mM, and then $D_{Bu_4N^+}$ becomes smaller than $D_{SDS(Bu)}$, indicating that almost all Bu$_4$N$^+$ ions are bound to the mixed micelle.

Figure 7 shows the fractions of TAA$^+$ ions in the micellar state as a function of SDS concentration. The populations of TAA$^+$ ions, which are bound with SDS to form the mixed micelles, exhibit a sigmoid growth trend. For the Bu$_4$NBr/SDS

Figure 7. Fraction of TAA$^+$ ions in the micellar state as a function of [SDS]. The populations of TAA$^+$ ions bound to the TAA-SDS mixed micelles show a sigmoid growth trend, suggesting that the association between TAA$^+$ ions and SDS strongly depends on SDS concentration.
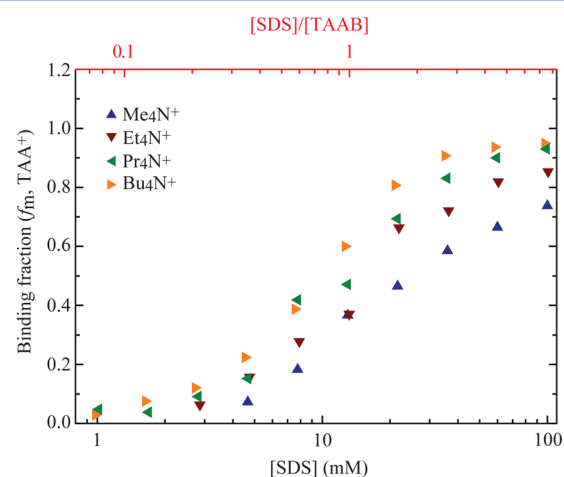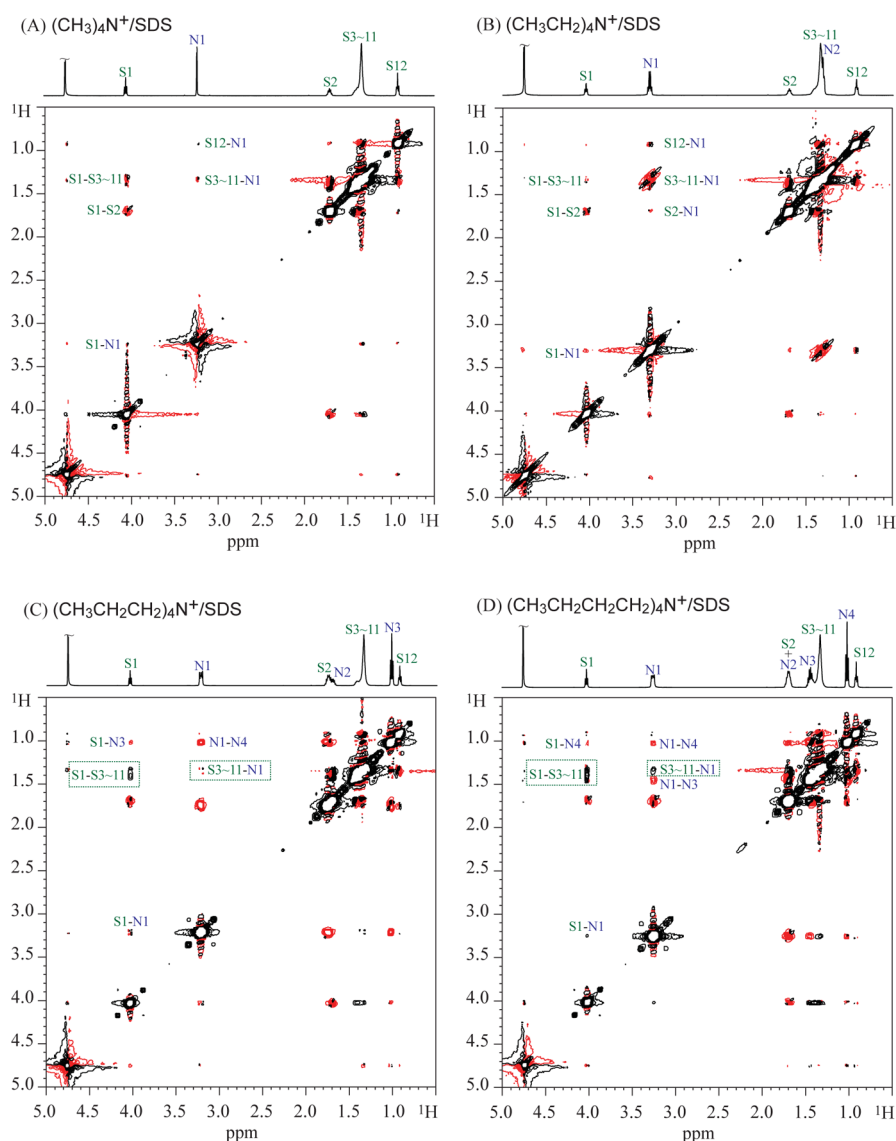
mixed micelle. This means that not all Me$_4$N$^+$ ions are bound tightly with the Me$_4$N-SDS mixed micelles even when the number of binding sites on the mixed micelles is much larger than the number of Me$_4$N$^+$ ions. The self-diffusion behavior of the Et$_4$NBr/SDS system is similar to that of the Me$_4$NBr/SDS system.

For the SDS solutions containing the more hydrophobic Bu$_4$NBr and Pr$_4$NBr, the self-diffusion behavior is quite different from that of SDS solutions with added Me$_4$NBr and Et$_4$NBr. The Bu$_4$NBr/SDS system is used as an example to demonstrate the self-diffusion behavior. In Figure 6, $D_{SDS(Bu)}$

Figure 8. 2D NOESY NMR spectra of the four TAAB/SDS solutions obtained with a 200 ms mixing time: (A) Me_4NBr/SDS, (B) Et_4NBr/SDS, (C) Pr_4NBr/SDS, and (D) Bu_4NBr/SDS. [TAAB] = 13.2 mM and [SDS] = 25 mM. The contour levels in the spectra are linearly spaced. (C, D) Positive and negative NOE cross-peaks are observed. The negative NOE cross-peaks (black contour lines) are framed within rectangles on one side of the diagonal.

solution, as an example, the binding fraction of Bu_4NBr rises slowly when [SDS] < 5 mM. The number of micellar bound Bu_4N^+ ions goes through a rapid growth phase when 5 mM < [SDS] < 20 mM and then levels off when [SDS] > 20 mM. This suggests that the association between TAA$^+$ ions and SDS strongly depends on the SDS concentration. The maximum fractions of micelle-bound TAA$^+$ ions are 0.74 for Me_4N^+, 0.86 for Et_4N^+, 0.93 for Pr_4N^+, and 0.95 for Bu_4N^+. These results are not surprising considering the hydrophobic nature of all four alkyl ammonium ions.

Location of TAA$^+$ Ions in Mixed Micelles from 2D NOESY NMR. As stated in the previous sections, TAA$^+$ ions associate with SDS to form mixed micelles. The formation of the mixed micelles is directly evident from intermolecular NOESY interactions between TAA$^+$ ions and SDS. In order to avoid spin diffusion problems, the mixing time was set to 200 ms, which is shorter than the typical mixing time (>500 ms) used for the small-molecule sample. Figure 8A–D shows the 2D ^{1}H–^{1}H NOESY spectra of the four mixed TAAB/SDS/

D$_2$O solutions ([TAAB] = 13.2 mM and [SDS] = 25.0 mM). Generally, for all four TAAB/SDS systems, there are strong correlations between S3–11 protons and N1 protons, indicating that TAA$^+$ ions and SDS are within close enough proximity to permit interactions. The observation also suggests that TAA$^+$ ions are not only attached to the micellar surface but are also inserted into the micellar interior. Thus, in the presence of TAABs, TAA$^+$ ions and SDS form mixed micelles and TAA$^+$ ions constitute a part of the hydrophobic core of the mixed micelle. More specifically, for the Me_4NBr/SDS and Et_4NBr/SDS solutions, there are clear cross-peaks between S12 and N1, indicating that Me_4N^+ and Et_4N^+ might be located in the center of the mixed micelle. However, for the Pr_4NBr/SDS and Bu_4NBr/SDS solutions, the S12−N1 cross-peaks are indistinct. This indicates that Pr_4N^+ and Bu_4N^+ are not located in the center of the mixed micelles, which is due to their large ionic sizes.

The most interesting feature in the 2D NOESY spectra is that for the Pr_4NBr/SDS and Bu_4NBr/SDS solutions, positive

and negative nuclear Overhauser effects (NOE) are simultaneously observed. In the case of the Bu$_4$NBr/SDS solution (Figure 8D), for example, the phase of the cross-peaks between S1 protons and Bu$_4$N$^+$ (N4 protons) is opposite to the phase of diagonal peaks (positive NOE); however, the phases of the cross-peaks and the diagonal peaks for the S1 protons and S3−11 protons are the same (negative NOE). Also, S3−11−N1 NOE is negative. In contrast, the phases of the cross-peaks of all protons in the 2D NOESY spectra for the Me$_4$NBr/SDS and Et$_4$NBr/SDS solutions are opposite to those of the corresponding diagonal peaks.

In principle, positive and negative NOE correspond to the local motion of spins on the short ($\omega^2 \tau_c^2 < 1$) and the long ($\omega^2 \tau_c^2 > 1$) sides of the extreme narrowing limit, respectively, where ω is the spectrometer frequency and τ_c is the correlation time for reorientation of the spin. For small molecules like SDS in a dilution solution, the molecular tumbling rate is very fast and positive NOE is expected. Tzeng and Hou[47] have found that SDS molecules in the micellar state show positive NOE, indicating that SDS molecules in the pure SDS micelles possess a rotational correlation times shorter than the critical correlation time ($\tau_{c,crit} = |\sqrt{5}/2\omega^0|$, ω^0 is the nuclear Larmor frequency in rad s^{-1}). Moreover, the addition of NaCl (13.2 mM) or NH$_4$Br (13.2 mM) into the SDS solution (25.0 mM) does not change the sign of NOE of SDS. The 2D NOESY spectra (Figure S1) of NaCl/SDS and NH$_4$Br/SDS solutions are given in the Supporting Information. Also, the molecular dynamics of SDS is not markedly affected by the added Me$_4$NBr, Et$_4$NBr, NaCl, and NH$_4$Br.

The signs of NOE among the protons of TAA$^+$ ions in the four TAAB/SDS mixed systems are all positive, indicating that the motion of TAA$^+$ ions are not restricted by the strong electrostatic interactions with SDS molecules. Additionally, the effective molecular weight of the TAA-SDS mixed micelles will be higher than several tens of thousands so that negative NOE is expected for the TAA$^+$ ions. However, by considering that most of the TAA$^+$ ions are only attached on the surface of the mixed micelles, the motion of TAA$^+$ ions can be very fast because they are still solvated by water.[48]

For the Pr$_4$NBr/SDS and Bu$_4$NBr/SDS solutions, the negative NOE (S1−S3∼S11) is shown among the alkyl chain protons, whereas positive NOE is observed between the S1 protons (α-CH$_2$) and the ammonium ions. The extremely different tumbling rate in the same molecule has been also found in polypeptides and dendrimers.[49−51] The negative NOE between S1 and S3−11 indicates that the motion of the alkyl segment of an SDS molecule is restricted. This might be attributed to Bu$_4$N$^+$ (or Pr$_4$N$^+$) being firmly attached to the alkyl chain of SDS in the mixed micelle. In addition, the electrostatic attractions between the ammonium ion and the sulfate group further bind them together.

■ CONCLUDING REMARKS

This study used pyrene solubilization and several NMR techniques to reveal how TAA$^+$ ions associate with SDS molecules to form mixed micelles. Pyrene is a versatile fluorescence probe for sensing the micropolarity within surfactant micelles. However, as charged species are present in the hydrophobic core of a micelle, the micropolarity inside the micelle sensed by pyrene might be deceptive. Nevertheless, the pyrene I_1/I_3 curves shown in Figure 2 still provide valuable information, such as the cmc of SDS for the TAAB/SDS systems. Besides, as [SDS] > cmc, the I_1/I_3 curves of the

TAAB/SDS solutions show discontinuous changes when the ratio of [SDS]/[TAAB] reaches certain values. This implies that there is an abrupt structural change of the mixed micelles at a certain SDS concentration. The discontinuous changes of the lower I_1/I_3 plateau values correspond to the inflection breaks in the plot of self-diffusion coefficients versus [SDS] (Figure 6) and the minimum ^{1}H chemical shift of SDS α-CH$_2$, which are the indications for the cmc-II of SDS with TAA$^+$ ions.

Proton chemical shift analysis provided experimental evidence of the hydration changes that accompany TAA$^+$ binding on the surface of the mixed micelles. The binding of TAA$^+$ ions decreases the water accessibility to the surface of the mixed micelles, which results in the upfield chemical shift of SDS α-CH$_2$. Thus, the chemical change could provide a convenient index for the degree of dehydration on the micellar surface. For anionic surfactant aqueous solutions, the cloud point (CP) phenomenon is considered to be closely related to hydrophobic character near the headgroup region.[15] The surface of a Bu$_4$N$^+$-SDS mixed micelle is extremely hydrophobic, which thus accounts for that CP phenomenon is commonly seen for the Bu$_4$NBr/SDS system.[14,15]

Analysis of the self-diffusion data indicates that the molar fraction of TAA$^+$ ions in the TAA-SDS mixed micelles can be as high as 0.8. Considering the larger ionic sizes of TAA$^+$ ions, most of TAA$^+$ ions must be attached on the surface or located in the palisade layer of the mixed micelles rather than being inserted into the central hydrophobic core. Our experimental results support a structural model, in which TAA$^+$ ions constitute a dense and compact layer around the surface of the mixed micelles. Moreover, some TAA$^+$ ions are bound on this primary layer to form a much looser layer.[17]

The results of NOESY experiments enabled the identification the explicit location of TAA$^+$ ions in the mixed micelles. The size of TAA$^+$ ions is an important factor in governing how the TAA$^+$ ions are incorporated with SDS molecules to form mixed micelles. For the Me$_4$NBr/SDS system, clear cross-peaks were observed between the terminal methyl protons (S12) of SDS and the methyl protons of Me$_4$N$^+$ (N1). This indicates that Me$_4$N$^+$ is located in the center of the mixed micelle even though Me$_4$N$^+$ has weak binding affinity to SDS molecules. Therefore, the NOE study suggests that Me$_4$N$^+$ does not only behave as the counterion, reducing the surface charges, but is also inserted into the hydrocarbon core of the micelle. This conclusion is somewhat different from the single-site interaction model based on a calorimetric study.[22] However, for the Pr$_4$NBr/SDS and Bu$_4$NBr/SDS systems, our results are in excellent agreement with a two-site binding model.[22] Furthermore, the size of Bu$_4$N$^+$ is comparable to that of the SDS molecule, and its shape is near spherical. The NOESY spectrum shows that Bu$_4$N$^+$ is not located in the core of the mixed micelles. This is reasonable because if Bu$_4$N$^+$ were located in the core, the hydrocarbon part of the mixed micelle would be very loose and energetically unfavorable. Finally, for the Pr$_4$NBr/SDS and Bu$_4$NBr/SDS systems, different tumbling rates were found among the SDS alkyl protons. This is the first time that simultaneous positive and negative NOE have been observed in simple micellar systems. Nevertheless, an understanding of the complex internal motion requires more detailed relaxation information on every carbon of the SDS alkyl chain.

■ ASSOCIATED CONTENT

S **Supporting Information**

The 2D NOESY spectra (Figure S1) of NaCl/SDS and NH$_4$Br/SDS solutions are provided. This material is available free of charge via the Internet at http://pubs.acs.org.

■ AUTHOR INFORMATION

Corresponding Author
*Tel.: +886-6-2757575, ext 62641. Fax: +886-6-2344496. E-mail: sshou@mail.ncku.edu.tw.

Notes

The authors declare no competing financial interest.

■ ACKNOWLEDGMENTS

■ REFERENCES

(1) Tadros, T. F. *Applied Surfactants: Principles and Applications*; Wiley-VCH Verlag GmbH & Co.: Weinheim, 2005.

(2) Kim, J.; Domach, M. M.; Tilton, R. D. Effect of Electrolytes on the Pyrene Solubilization Capacity of Dodecyl Sulfate Micelles. *Langmuir* **2000**, *16*, 10037−10043.

(3) Full, A. P.; Kaler, E. W.; Arellano, J.; Puig, J. E. Microemulsion Polymerization of Styrene: The Effect of Salt and Structure. *Macromolecules* **1996**, *29*, 2764−2775.

(4) Paria, S.; Khilar, K. C. A Review on Experimental Studies of Surfactant Adsorption at the Hydrophilic Solid−Water Interface. *Adv. Colloid Interface Sci.* **2004**, *110*, 75−95.

(5) Mukerjee, P.; Mysels, K. J.; Kapauan, P. Counterion Specificity in the Formation of Ionic Micelles-Size, Hydration, and Hydrophobic Bonding Effects. *J. Phys. Chem.* **1967**, *71*, 4166−4175.

(6) Goddard, E. D.; Harva, O.; Jones, T. G. The Effect of Univalent Cations on the Critical Micelle Concentration of Sodium Dodecyl Sulphate. *Trans. Faraday Soc.* **1953**, *49*, 980−984.

(7) Sein, A.; Engberts, J. B. F. N. Micelle to Lamellar Aggregate Transition of an Anionic Surfactant in Dilute Aqueous Solution Induced by Alkali Metal Chloride and Tetraalkylammonium Chloride Salts. *Langmuir* **1995**, *11*, 455−465.

(8) Mandal, A. B.; Wang, L.; Brown, K.; Verrall, R. E. Conductance and NMR Studies of Cetyltrimethylammonium Bromide and Chloride Micelles in the Presence of Several Additives. *J. Colloid Interface Sci.* **1993**, *161*, 292−299.

(9) Kanthimathi, M.; Deepa, K.; Nair, B. U.; Mandal, A. B. Fluorescence Quenching of Pyrene by Chromium Complexes in Sodium Dodecyl Sulfate Micelles. *Bull. Chem. Soc. Jpn.* **2000**, *73*, 1769−1775.

(10) James, J.; Ramalechume, C.; Mandal, A. B. Self-Diffusion Studies on PEO-PPO-PEO Triblock Copolymer Micelles in SDS Micelles and Vice Versa Using Cyclic Voltammetry. *Chem. Phys. Lett.* **2005**, *405*, 84−89.

(11) James, J.; Krishnan, R. S. G.; Samikannu, S.; Mandal, A. B. Interaction of Poly(ethylene oxide)-poly(propylene oxide)-poly-(ethylene oxide) Triblock Copolymer of Molecular Weight 2800 with Sodium Dodecylsulfate (SDS) Micelles: Some Physicochemical Studies. *Chem. Phys.* **2005**, *312*, 275−287.

(12) James, J.; Mandal, A. B. The Aggregation of Tyr-Phe Dipeptide and Val-Tyr-Val Tripeptide in Aqueous Solution and in the Presence of SDS and PEO-PPO-PEO Triblock Copolymer: Fluorescence Spectroscopic Studies. *J. Colloid Interface Sci.* **2011**, *360*, 600−605.

(13) Yu, Z.-J.; Xu, G. Physicochemical Properties of Aqueous Mixtures of Tetrabutylammonium Bromide and Anionic Surfactants. 1. Temperature-Induced Micellar Growth and Cloud Point Phenomenon. *J. Phys. Chem.* **1989**, *93*, 7441−7445.

(14) Mata, J.; Varade, D.; Ghosh, G.; Bahadur, P. Effect of Tetrabutylammonium Bromide on the Micelles of Sodium Dodecyl Sulfate. *Colloids Surf., A* **2004**, *245*, 69−73.

(15) Kumar, S.; Sharma, D.; Khan, Z. A.; ud-Din, K. Temperature-[Salt] Compensation for Clouding in Ionic Micellar Systems Containing Sodium Dodecyl Sulfate and Symmetrical Quaternary Bromides. *Langmuir* **2003**, *19*, 3539−3541.

(16) Bales, B. L.; Zana, R. Cloud Point of Aqueous Solutions of Tetrabutylammonium Dodecyl Sulfate Is a Function of the Concentration of Counterions in the Aqueous Phase. *Langmuir* **2004**, *20*, 1579−1581.

(17) Benrraou, M.; Bales, B. L.; Zana, R. Effect of the Nature of the Counterion on the Properties of Anionic Surfactants. 1. Cmc, Ionization Degree at the Cmc and Aggregation Number of Micelles of Sodium, Cesium, Tetramethylammonium, Tetraethylammonium, Tetrapropylammonium, and Tetrabutylammonium Dodecyl Sulfates. *J. Phys. Chem. B* **2003**, *107*, 13432−13440.

(18) Bales, B. L.; Tiguida, K.; Zana, R. Effect of the Nature of the Counterion on the Properties of Anionic Surfactants. 2. Aggregation Number-Based Micelle Ionization Degrees for Micelles of Tetraalky-lammonium Dodecylsulfates. *J. Phys. Chem. B* **2004**, *108*, 14948−14955.

(19) Zana, R.; Benrraou, M.; Bales, B. L. Effect of the Nature of the Counterion on the Properties of Anionic Surfactants. 3. Self-Association Behavior of Tetrabutylammonium Dodecyl Sulfate and Tetradecyl Sulfate: Clouding and Micellar Growth. *J. Phys. Chem. B* **2004**, *108*, 18195−18203.

(20) Bales, B. L.; Benrraou, M.; Tiguida, K.; Zana, R. Effect of the Nature of the Counterion on the Properties of Anionic Surfactants. 4. Characterizing Micelles of Tetraalkylammonium Dodecyl Sulfate as Reaction Media. *J. Phys. Chem. B* **2005**, *109*, 7987−7997.

(21) Paul, A.; Griffiths, P. C.; Pettersson, E.; Stilbs, P.; Bales, B. L.; Zana, R.; Heenan, R. K. Nuclear Magnetic Resonance and Small-Angle Neutron Scattering Studies of Anionic Surfactants with Macro-counterions: Tetramethylammonium Dodecyl Sulfate. *J. Phys. Chem. B* **2005**, *109*, 15775−15779.

(22) Mitra, D.; Chakraborty, I.; Bhattacharya, S. C.; Moulik, S. P. Interfacial and Solution Properties of Tetraalkylammonium Bromides and their Sodium Dodecyl Sulfate Interacted Products: A Detailed Physicochemical Study. *Langmuir* **2007**, *23*, 3049−3061.

(23) Das, C.; Das, B. Effect of Tetraalkylammonium Salts on the Micellar Behavior of Lithium Dodecyl Sulfate: A Conductometric and Tensiometric Study. *J. Mol. Liq.* **2008**, *137*, 152−158.

(24) Ali, M.; Chakraborty, A.; Bardhan, S.; Saha, S. K. Thermodynamics of Micellization of Ammoniumdodecyl Sulfate in Aqueous Solutions of Symmetrical Tetraalkylammonium Bromides: Clouding in Presence of Tetrabutylammonium Bromide Salt. *J. Dispersion Sci. Technol.* **2010**, *31*, 1220−1229.

(25) Nightingale, E. R. Phenomenological Theory of Ion Solvation. Effective Radii of Hydrated Ions. *J. Phys. Chem.* **1959**, *63*, 1381−1387.

(26) Wu, D.; Chen, A.; Johnson, C. S., Jr. An Improved Diffusion-Ordered Spectroscopy Experiment Incorporating Bipolar-Gradient Pulses. *J. Magn. Reson.* **1995**, *115*, 260−264.

(27) Wirth, H. E. Equilibria in Solutions of Tetraalkylammonium Bromides. *J. Phys. Chem.* **1967**, *71*, 2922−2929.

(28) Blandamer, M. J.; Foster, M. J.; Hidden, N. J.; Symons, M. C. R. Ultrasonic Absorption Properties of Solutions. *Trans. Faraday Soc.* **1968**, *64*, 3247−3254.

(29) Maitia, K.; Bhattacharyaa, S. C.; Moulik, S. P.; Panda, A. K. Physicochemistry of the Binary Interacting Mixtures of Cetylpyr-idinium Chloride (CPC) and Sodium Dodecylsulfate (SDS) with Special Reference to the Catanionic Ion-Pair (Coacervate) Behavior. *Colloids Surf., A* **2010**, *355*, 88−98.

(30) Lianos, P.; Zana, R.; Viriot, M. Study of the Solubilization of Aromatic Hydrocarbons by Aqueous Micellar Solutions. *J. Phys. Chem.* **1984**, *88*, 1098−1101.

(31) Bacaloglu, R.; Bunton, C.; Ortega, F. Micellar Enhancements of Rates of S$_N$2 Reactions of Halide Ions. The Effect of Headgroup Size. *J. Phys. Chem.* **1989**, *93*, 1497−1502.

(32) Sabaté, R.; Gallardo, M.; Esterlich, J. Location of Pinacyanol in Micellar Solutions of N-Alkyl Trimethylammonium Bromide Surfactants. *J. Colloid Interface Sci.* **2001**, *233*, 205−210.

(33) Amato, M. E.; Caponetti, E.; Martino, D. C.; Pedone, L. ¹H and ¹⁹F NMR Investigation on Mixed Hydrocarbon-Fluorocarbon Micelles. *J. Phys. Chem. B* **2003**, *107*, 10048−10056.

(34) Funasaki, N.; Ishikawa, S.; Neya, S. 1:1 and 1:2 Complexes Between Long-Chain Surfactant and α-cyclodextrin Studied by NMR. *J. Phys. Chem. B* **2004**, *108*, 9593−9598.

(35) Nordstierna, L.; Furo, I.; Stilbs, P. Mixed Micelles of Fluorinated and Hydrogenated Surfactants. *J. Am. Chem. Soc.* **2006**, *128*, 6704.

(36) Cui, X.; Mao, S.; Liu, M.; Yuan, H.; Du, Y. Mechanism of Surfactant Micelle Formation. *Langmuir* **2008**, *24*, 10771−10775.

(37) Cui, X. H.; Jiang, Y.; Yang, C. S.; Lu, X. Y.; Chen, H.; Mao, S. Z.; Liu, M. L.; Yuan, H. Z; Luo, P. Y.; Du, Y. R. Mechanism of the Mixed Surfactant Micelle Formation. *J. Phys. Chem. B* **2010**, *114*, 7808−7816.

(38) Huibers, P. D. T. Quantum-Chemical Calculations of the Charge Distribution in Ionic Surfactants. *Langmuir* **1999**, *15*, 7546−7550.

(39) Phani Kumar, B. V. N.; Priyadharsini, S. U.; Prameela, G. K. S.; Mandal, A. B. NMR Investigation of Self-Aggregation Characteristics of SDS in a Model Assembled Tri-Block Copolymer Solution. *J. Colloid Interface Sci.* **2011**, *360*, 154−162.

(40) Pan, A.; Naskar, B.; Prameela, G. K. S.; Phani Kumar, B. V. N.; Mandal, A. B.; Bhattacharya, S. C.; Moulik, S. P. Amphiphile Behavior in Mixed Solvent Media I: Self-Aggregation and Ion Association of Sodium Dodecylsulfate in 1,4-Dioxane−Water and Methanol−Water Media. *Langmuir* **2012**, *28*, 13830−13843.

(41) Orfi, L.; Lin, M.; Larive, C. K. Measurement of SDS Micelle-Peptide Association Using ¹H NMR Chemical Shift Analysis and Pulsed-Field Gradient NMR Spectroscopy. *Anal. Chem.* **1998**, *70*, 1339−45.

(42) Mandal, A. B.; Nair, B. U. Cyclic Voltammetric Technique for the Determination of the Critical Micelle Concentration, Self-Diffusion Coefficient of Micelles, and Partition Coefficient of an Electrochemical Probe. *J. Phys. Chem.* **1991**, *95*, 9008−9013.

(43) Geetha, B.; Mandal, A. B. Self-Diffusion Studies on ω-Methoxy Polyethylene Glycol Macromomer Micelles by Using Cyclic Voltammetric and Fourier Transform Pulsed Gradient Spin-Echo Nuclear Magnetic Resonance Techniques. *Langmuir* **1995**, *11*, 1464−1467.

(44) Stilbs, P.; Lindman, B. Determination of Organic Counterion Binding to Micelles Through Fourier Transform NMR Self-Diffusion Measurements. *J. Phys. Chem.* **1981**, *85*, 2587−2589.

(45) Stilbs, P. Fourier Transform Pulsed-Gradient Spin-Echo Studies of Molecular Diffusion. *Prog. Nucl. Magn. Reson. Spectrosc.* **1987**, *19*, 1−45.

(46) González-Pérez, A.; Ruso, J. M.; Prieto, G.; Sarmiento, F. Structural Micellar Transition for Fluorinated and Hydrogenated Sodium Carboxylates Induced by Solubilization of Benzyl Alcohol. *Langmuir* **2004**, *20*, 8476−8481.

(47) Tzeng, J.-K.; Hou, S.-S. Interactions between Poly(N-vinyl-formamide) and Sodium Dodecyl Sulfate as Studied by Fluorescence and Two-Dimensional NOE NMR Spectroscopy. *Macromolecules* **2008**, *41*, 1281−1288.

(48) Jayakumar, R.; Jeevan, R. G.; Mandal, A. B. Aggregation, Hydrogen Bonding and Thermodynamic Studies on Boc-Val-Val-Ile-OMe Tripeptide Mecelles in Chloroform. *J. Chem. Soc., Faraday Trans.* **1994**, *90*, 2725−2730.

(49) Uma, K.; Balaram, H.; Raghothama, S.; Balaram, P. Simultaneous Observation of Positive and Negative Nuclear Over-hauser Effects in Oligopeptides due to Segmental Motion. *Biochem. Biophys. Res. Commun.* **1988**, *151*, 153−157.

(50) Krishman, V. V.; Shekar, S. C.; Kumar, A. Simultaneous Observation of Positive and Negative NOE in Biomolecules: A Bistable Jump Model for Segmental Motion with Modulation of Internuclear Distances. *J. Am. Chem. Soc.* **1991**, *113*, 7542−7550.

(51) Chai, M.; Niu, Y.; Youngs, W. J.; Rinaldi, P. L. Structure and Conformation of DAB Dendrimers in Solution via Multidimensional NMR Techniques. *J. Am. Chem. Soc.* **2001**, *123*, 4670−4678.